Coupled Multiphysics and Chemistry Simulations of PCR Microreactors with Active Control

M. M. Athavale, Z.J. Chen, M. Furmanczyk, and A. J. Przekwas
CFD Research Corp., 215 Wynn Drive, Huntsville, AL 35805, USA
mma@cfdrc.com, Ph: (256)726-4817, fax: (256)726-4806

ABSTRACT

High-fidelity simulation tools that couple fluid flow, heat transfer and chemistry of PCR microreactors have been applied to different microreactor designs. The tools are coupled to a controller software for thermal control of the virtual reactors. The numerical tools can be used for comprehensive simulations of PCR microreactors for assessment of DNA amplification, control and uniformity of temperature and can be used to optimize reactor geometry, heater/cooler placement and to generate controller schedules. Results for different PCR reactor designs are presented and demonstrate the capability of such tools and their utility during the design phase.

Keywords: Multiphysics Numerical methods, DNA amplification, PCR microreactors, PCR thermal control

INTRODUCTION AND OBJECTIVES

Microreactors for PCR amplification form an important part of on-chip DNA analysis systems. Reduction in the reactor size offers numerous advantages over the conventional PCR reactors. The sample sizes in microreactors are small (micro-nano liter range) which reduces the consumption of reagents. More importantly, the smaller sized samples can be heated and cooled much more rapidly than conventional reactors. This results in much shorter cycle times for amplification cycles of PCR. Micro reactors can be easily integrated with heating and cooling elements in a lab-on-chip. One drawback of the microreactors is that their small sizes make the process of thermal sensing and control difficult. Since the PCR processes are very sensitive to temperatures, precise information of the temperature in the reactor and temperature control become critical to the success of a PCR microreactor.

Present day numerical simulation tools offer a way to assess the details of the flow, thermal and chemical processes that take place in the microreactors. These tools can also be integrated with appropriate controlling software to provide controller schedules for optimum reactor performance. CFDRC has developed CFD-ACE+MEMS, a multi-physics numerical code for high-fidelity thermo-fluid simulations of MEMS and this has been recently extended to include the chemical reactions that take place during PCR amplification. The multi-physics software has also been linked with an LQT-based controller software for temperature control of the 'virtual reactor' through variations in the applied heater and cooling powers. This comprehensive tool set has been applied to different reactor designs 1. Thermal control of a single well PCR reactor; 2. Flow+thermal+chemistry simulations in a traveling sample PCR microreactor; and 3. Flow+thermal+chemistry simulations of a continuous flow microreactor. Presented here are details of the first two cases.

DESCRIPTION OF THE NUMERICAL TOOLS

Fluid and thermal Solver: The design tool, CFD-ACE+MEMS consists of a multiphysics solver, which is used to solve flow, thermal and other coupled physics such as chemical reactions [1]. The flow and thermal solver employs a pressure-based algorithm on unstructured-/hybrid/adaptive meshes for integration of Navier-Stokes flow equations. Salient features of the solver relevant to the current applications include incompressible and compressible flows, steady and time-accurate simulations, coupled flow+thermal+chemistry simulations, moving and deforming grid formulation, arbitrary, sliding interface methodology and conjugate heat transfer. The chemistry modeling capabilities include volume and surface reactions, multi-step chemistry, finite rate and infinite rate chemistry, coupling with thermal and flow effects, and variable rate coefficients. The fluids and thermal solver has been extensively tested and validated on various MEMS, microfluidic and bio-MEMS devices.

Link with an LQT Controller: The controller software in the commercial package SABER [2] was linked with CFD-ACE+MEMS for control of the heaters and coolers used in PCR microreactors. The controller schematic in SABER is shown in Figure 2, where a CFD-ACE+ model represents the microreactor (plant). The requested time-temperature profile is input to the Linear Quadratic Tracker (LQT) in the SABER package. A feedback loop is added for tighter temperature control required in the PCR process and to avoid over- and under-shoots during temperature ramping.

PCR reaction model: The overall process of PCR amplification is complex, and very few descriptions of the chemical reactions that form the various steps of PCR are available in the literature. Recently, a detailed, engineering chemistry model for PCR was proposed by Hunicke-Smith [3] which describes the chemical reactions in the three major steps in PCR: denaturing, annealing and extension. A total of five major chemical species are assumed to control the reactions: double-stranded DNA (dsDNA), or s_1s_2, its single strands (ssDNA), s_1 and s_2 and the primer-ssDNA complexes s_1p_2 and s_2p_1. These complexes are then extended to dsDNA in the extension step. The overall model thus consists of five major reaction sets as denoted below:

$$\begin{aligned} s_1s_2 &\xrightleftharpoons{k_D^+,k_D^-} s_1 + s_2 \\ s_1 + p_2 &\xrightleftharpoons{k_A^+,k_A^-} s_1p_2 \\ p_1 + s_2 &\xrightleftharpoons{k_A^+,k_A^-} p_1s_2 \\ s_1p_2 &\xrightarrow{k_E} s_1s_2 \\ p_1s_2 &\xrightarrow{k_E} s_1s_2 \end{aligned} \qquad (1)$$

The first reaction denotes the denaturation of the dsDNA. Second and third reactions relate to the annealing step where primer-ssDNA duplexes are formed, and the last two reactions form the extension stage. Although the reaction involving s_2p_1 was not included in the original model, it is included here and the reaction rates are assumed to be the same for both annealing reactions. Each of the reactions is taken to proceed at finite rates denoted in each of these reactions. The time rates of change of concentrations of each of the five species are then given as:

$$\begin{aligned} \frac{d[s_1]}{dt} &= k_D^+[s_1s_2] + k_A^-[s_1p_2] - k_D^-[s_1][s_2] - k_A^+[s_1] \\ \frac{d[s_2]}{dt} &= k_D^+[s_1s_2] + k_A^-[p_1s_2] - k_D^-[s_1][s_2] - k_A^+[s_2] \\ \frac{d[s_1p_2]}{dt} &= k_A^+[s_1] - k_A^-[s_1p_2] - k_E[s_1p_2] \\ \frac{d[p_1s_2]}{dt} &= k_A^+[s_2] - k_A^-[p_1s_2] - k_E[p_1s_2] \\ \frac{d[s_1s_2]}{dt} &= k_E[s_1p_2] + k_E[p_1s_2] - k_D^+[s_1s_2] + k_D^-[s_1][s_2] \end{aligned} \qquad (2)$$

The various rate constants that enter in these equations are primarily functions of temperature. Based on the observed characteristics of the reactions the proposed rate constant expressions are:

$$\begin{aligned} k_E &= 0.32_s{}^{-1} e^{-\left(T-70^oC\right)^2/\left(5^oC\right)^2} \\ k_A^+(T) &= 0.26_s{}^{-1}\,\frac{1+\tanh\left(-\left(T-62.5^oC\right)/5^oC\right)}{2} \\ k_A^-(T) &= 1.0_s{}^{-1}\,\frac{1+\tanh\left(\left(T-66^oC\right)/5^oC\right)}{2} \\ k_D^-(T) &= 1.0_s{}^{-1}\,\frac{1+\tanh\left(\left(T-88^oC\right)/5^oC\right)}{2} \\ k_D^-(T) &= 0.03_s{}^{-1}M\,\frac{1+\tanh\left(-\left(T-75^oC\right)/5^oC\right)}{2} \end{aligned} \qquad (3)$$

The rate constants for forward and reverse reactions in denaturation and annealing steps have a very sharp transition point, where the rates change from minimum (maximum) values to maximum (minimum) values over a 5 degree temperature change. The rate constant for the extension step, however, has a sharp peak at a reference temperature and drops off rapidly at higher and lower temperatures.

This PCR chemistry model has been included in CFD-ACE+MEMS and is coupled with the flow and thermal fields. Concentration of each of the species in the reactor is calculated using standard convective-diffusive transport equations with appropriate source and sink terms derived from the rate equations (Eqn. 3) for each of the species.

NUMERICAL SIMULATIONS

Three examples of thermal-fluidics-control-chemistry for PCR reactors were completed, and results from only two of them are presented (for lack of space) below to show the capability of the overall numerical simulation tool.

1. Thermal-Fluidic-Controls simulations of a stationary sample reactor: A schematic of the single well reactor described in [4] is shown in Figure 1. It has a stationary sample in a circular well. Heating is achieved via the coil heater, and the reactor base is actively cooled to produce PCR thermal cycling. The CFD-ACE+ model represents the actual reactor (plant), and the controller software controls the heater and cooler power levels to produce desired time-temperature profiles. Figure 2 shows a schematic of the controller software and the connections with the plant. Finally, Figure 3 shows a typical thermal cycle response generated with the coupled software, also shown is the desired response, and the simulated profile is seen to match the desired profile very closely, with very small over/undershoots.

2. Flow+thermal+chemistry calculations in a shuttling sample PCR reactor: This reactor was proposed in Ref 3. and consists of a straight tube with three heaters mounted on the tube to provide regions of different temperatures as shown in Figure 4. The sample is in the form of a plug

with air on either side, and is moved back-and-forth under the three heaters to generate thermal cycling. Time accurate simulations were performed with a moving grid algorithm to account for sample motion. Sample interface with the tube wall was treated through an arbitrary, sliding interface methodology. The cycle starts at the end of the denaturation stage with the sample at the leftmost heater. It is translated to annealing heater (extreme right) in 4 s., held for 10 s., translated back to extension heater (center) in 2 s., held for 20 s., moved to the left heater in 2 s., and held for 10 s for denaturation, which completes one cycle.

The variation in the sample center temperature as a function of time is shown in Figure 5. Calculated sample temperature fields show a fair amount of nonuniformity (over 2 C). Field plots of s_1s_2 and s_1p_2 concentrations at several different are shown in Figures 6 and 7. Starting with an s_1s_2 concentration of 1.e-7 mole, Figure 6a shows very small amounts of s_1s_2 after denaturation, which stays low till the extension stage (Fig. 6b), where the concentration slowly builds to about 1.86 times the initial concentration (Fig. 6c). Corresponding plots for the s_1p_2 complex are shown in Figure 7a-c, where starting with a low concentration after denaturation (Fig 7a), it builds up in annealing stage (Fig. 7b) and the complex is depleted in extension stage (Fig. 7c) as it is extended to generate s_1s_2.

Simulations show that the motion of the sample in the tube sets up recirculation patterns, which provide a degree of mixing and a mechanism for evening out the temperature. Evidence of this recirculation is also clearly seen in Figs. 6 and 7 where the contours are not parallel to the tube axis as would be in case of a stationary sample.

A continuous flow microreactor, described by Kopp et.al.[4], was also analyzed. Thermal field details are presented in Ref. 5. Flow+thermal+chemistry simulations on this reactor were also carried out and will be presented in the poster session.

SUMMARY

An engineering model for PCR chemistry has been incorporated into a fluid-thermal analysis software for detailed fluid-thermal-chemistry analysis of PCR reactors. The engineering model was tested on two microreactor geometries and produced reasonable results in terms of temperature fields and DNA amplification factors. The software also has been linked with controller software for virtual prototyping of PCR reactors and was used successfully on a stationary sample PCR microreactor to develop the heating/cooling powers and scheduling needed for precise control of sample temperature. The software provides a very unique and powerful capability for performance analysis, controller function and device optimization of PCR microreactors. The numerical tool provides a framework for the PCR chemistry coupled with the thermal and flowfields. Further work is needed on consolidation of the chemistry model, determination of realistic rate coefficients and/or addition of relevant species that may participate in the reactions; work is also in progress on validation of the model.

REFERENCES

1. CFD-ACE+ Users' Manual, CFD Research Corp., 2000.
2. MAST Reference Manual, Release 5.0, Analogy Inc., Beaverton, OR, 1999.
3. Hunicke-Smith, S.P., "PCR and Cycle Sequencng Reactions: A New Device and Engineering Model," Ph.D. Thesis, Stanford University, May 1997.
4. Yu, H. et.al., "A Miniaturized and Integrated Plastic Thermal Chemical Reactor for Genetic Analysis," Micro Total Analysis System (μ-TAS) 2000, pp.545-548.
5. Kopp, M.U., de Mello, A.J., and Manz, A., "Chemical Amplification: Continuous-flow PCR on a Chip," *Science*, vol. 280, pp. 1046, 1998.
6. Przekwas, A.J., Makhijani, V.B., Athavale, M.M., Klein, A. and Bartsch, P., "Computational Simulation of Bio-Microfluidic Processes in Integrated DNA Biochips," Micro Total Analysis System 2000, pp.561-564.

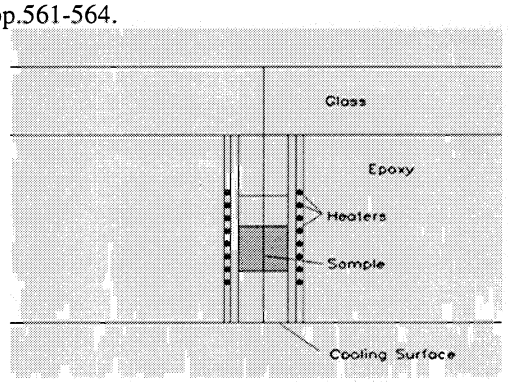

Figure 1. Schematic of a single well PCR microreactor

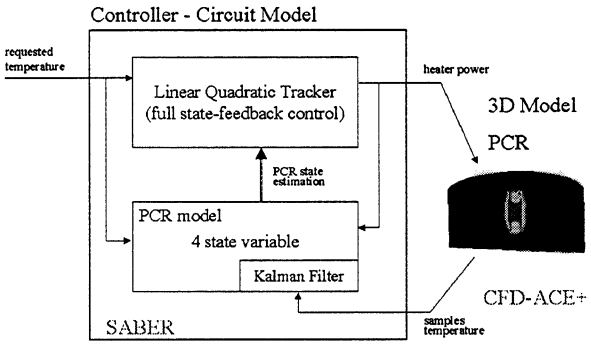

Figure 2. Description of the controller and link with virtual microreactor

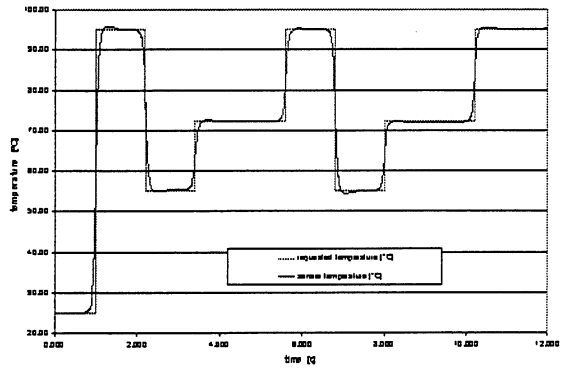

Figure 3. Calculated sample temperature profile shown with the requested profile.

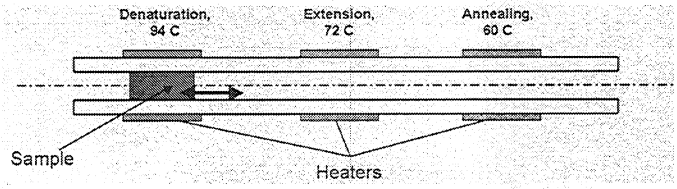

Figure 4. Schematic of a shuttling sample PCR reactor

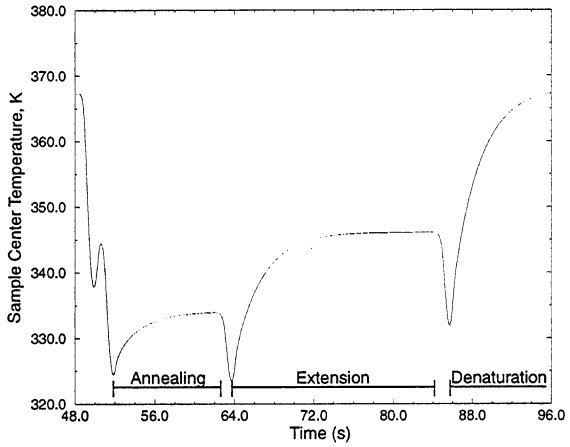

Figure 5. Time-temperature profile at the center of the shuttling sample.

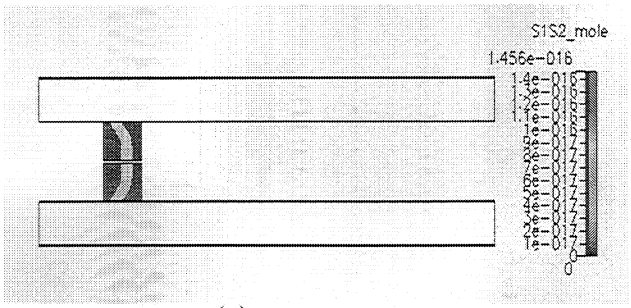

(a) end of denaturation

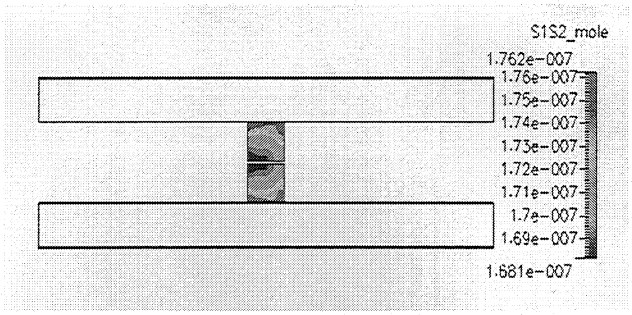

(b) halfway in extension

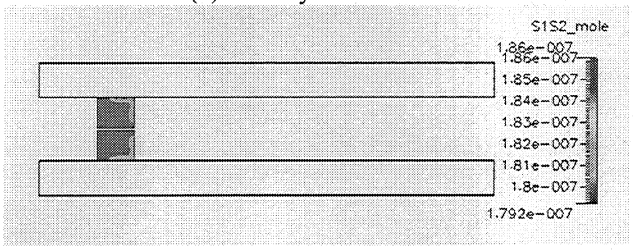

(c) end of extension stage

Figure 6. Concentration of dsDNA at different times

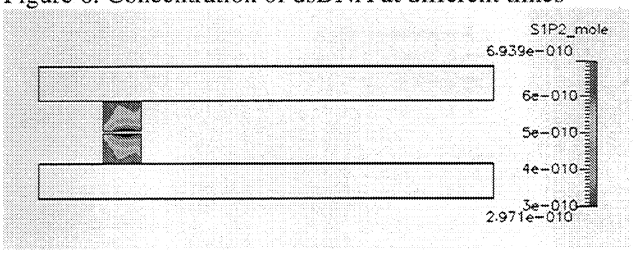

(a) end of denaturation

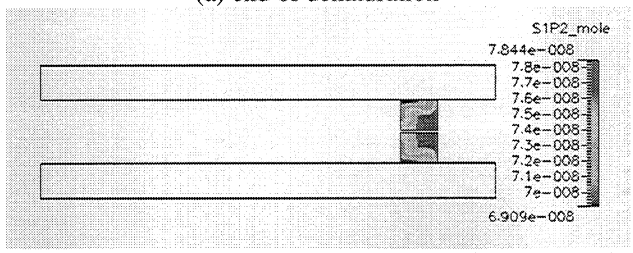

(b) halfway in annealing

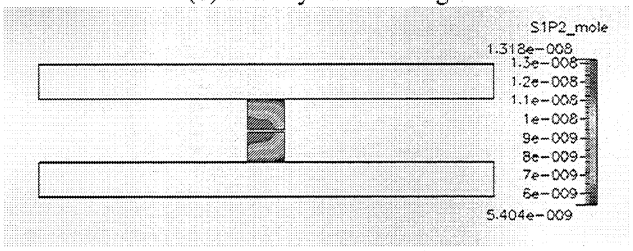

(c) halfway in extension stage

Figure 7. Concentration of the complex s_1p_2 at different times. Compare results in (c) with figure 6b.